Abstracts for the Society of Nuclear Medicine and Molecular Imaging, Greater New York and New England Chapters, 32nd Annual Northeast Regional Scientific Meeting, Newport, RI, October 26-28, 2018

Do Antidepressant Medications Affect Gastric Emptying Studies?*

Fritzgerald C Leveque LNMT, Maria-Bernadette S Tomas MD, Jeannine Drury LNMT, Alexis Schneiderman, Chris Pietrafesa, Kenneth J Nichols PhD, Christopher J Palestro MD.
Donald and Barbara Zucker School of Medicine at Hofstra/Northwell, New Hyde Park, NY.

Objectives: Even though antidepressants (ADs) are not among the list of contraindicated medications for pts undergoing gastric emptying scintigraphy, some are known to be associated with gastric side effects. Our study was undertaken to determine whether ADs are associated with unusual findings among pts undergoing gastric emptying scans, & to identify which specific classes of ADs are involved.

Methods: Data were examined for 407 pts (age = 51±19 years; 286 female; 121 male) referred for evaluation of gastric symptoms who underwent gastric motility studies. Only pts for whom the file notes detailed which AD was in use, or whose chart indicated no ADs, were included in this study. No pt had diabetes. For evaluation of liquid gastric emptying, dynamic imaging of the stomach was performed for 30 min following ingestion of 7.4 MBq ^{111}In-DTPA in 10 mL water immediately followed by 300 cc water, & computing the $T_{1/2}$ of liquid gastric emptying. Abnormal liquid emptying was defined as $T_{1/2}$ > 20 min. Evaluation of solid gastric emptying was performed for 4 hrs following ingestion of a standardized meal consisting of 4 ounces of egg whites labeled with 37 MBq ^{99m}Tc-sulfur colloid, along with 2 pieces of bread & 4 grams of jam. Simultaneous 1-min anterior & posterior static images were collected with pts erect. Attenuation-corrected conjugate view counts were determined within manually drawn regions over the stomach, & % retention values recorded at 1-hr intervals for 4 hrs. Abnormal solid emptying was defined as > 10% gastric retention at 4 hrs.

Results: 100 pts were on ADs & 307 were not. The % of male pts was similar for pts on & off ADs (31% versus 26%, p = 0.34), & ages were similar for pts on & off ADs (52±17 versus 51±19 years, p = 0.67). Of pts on ADs, 69 were on atypical ADs, mainly gamma-amino butyric acid receptor agonists (GABAAs), & the remaining 27 pts were on traditional ADs: 5 pts were on tricyclic ADs, 13 were on selective serotonin reuptake inhibitors, & 9 were on serotonin & norepinephrine reuptake inhibitors. Compared to pts not on ADs who had normal liquid emptying, liquid $T_{1/2}$ was slower for pts on GABAAs (21±21 versus 13±15 min, p = 0.01), but similar for those on traditional ADs (14±9 min, p = 0.79). Pts not on ADs with normal solid emptying had % solid retention of 5±2%, compared to which pts on GABAAs & those on traditional ADs had significantly higher solid retention of 10±14% & 13±19%, respectively (ANOVA F-statistic = 15.0, p < 0.001).

Conclusions: Further studies of the effects of ADs on gastric motility are warranted, as our results suggest that some antidepressants may retard liquid &/or solid emptying in pts referred for gastric emptying assessment.

*First Prize - Dr. Hussein M. Abdel-Dayem Award

Criteria-Based, Quantitative Evaluation of FDG-PET for the Diagnosis of Frontotemporal Lobar Degeneration *

[1]Jeremy Ford,MD MBA, [1]Shannon Glynn, [2]Silky Pahlajani MD, [1]Jana Ivanidze MD PhD
NewYork-Presbyterian, Weill Cornell Medical Center, New York, NY; [1]Department of Radiology; [2]Department of Neurology, New York, NY

Background: Frontotemporal Lobar Degeneration (FTLD) is a spectrum of disorders including frontotemporal dementia (FTD) and primary progressive aphasia (PPA). FDG-PET is instrumental in diagnosing FTLD; however, differentiation of FTLD from disease (AD) can often be challenging using qualitative analysis alone. Statistical Parametric Mapping (SPM) of FDG-PET studies, in which standardized uptake values (SUVs) within select regions are compared to a normal subject database, improves accuracy in diagnosing FTLD. However, there is a lack of well-defined quantitative criteria for the analysis of SPM data. The purpose of this study was to retrospectively evaluate the utility of SPM using pre-defined quantitative criteria and to explore metabolic patterns associated with FTLD disorders.

Methods: Thirty-one subjects in whom FTLD was clinically suspected were identified retrospectively using a searchable radiology database. FDG-PET data were post-processed using Siemens syngo.via software, comparing subjects' FDG-PET to a dataset derived from 33 healthy controls. An output t-score was generated for each region denoting the number of standard deviations difference from the healthy cohort. The clinical neurologic diagnosis was considered the gold standard. The concordance rate of qualitative review (based on the clinical radiology report) and the SPM method relative to the most recent neurological diagnosis was evaluated using the criteria outlined in Figure 2. Mann-Whitney U tests determined statistical significance of differences in region-specific metabolic activity between clinical subgroups.

Results: The concordance rate between the qualitative imaging and neurologic diagnoses was 65%, with 6% of radiologic impressions being indeterminate. SPM with whole brain normalization and pre-defined quantitative criteria demonstrated a higher rate of concordance (68%), with zero indeterminate cases. SPM with cerebellar normalization had the lowest concordance rate (61%). Relative to normal/MCI subjects, patients with PPA and FTD demonstrated decreased FDG avidity in the frontal lobes, the temporal poles, and the anterior cingulate, whereas patients with AD demonstrated decreased FDG avidity in posterior parietal structures and precuneus. Patients with neurologically diagnosed PPA exhibited a unique pattern of FDG avidity relative to MCI/Normal subjects, including increased FDG avidity in the bilateral occipital lobes (left, $p = 0.0082$; right, $p = 0.0160$). Findings remained robust following repeat analysis using cerebellar normalization ($p = 0.048$).

Conclusions: In this retrospective analysis, SPM with whole brain normalization and pre-defined quantitative criteria outperformed qualitative reads and SPM with cerebellar normalization in the workup of suspected FTLD. The major limitation of this study includes using heterogeneous clinical reference as the gold standard. SPM analysis demonstrated statistically significant differences relative to normal/MCI subjects, and subjects with a neurologic diagnosis of PPA had significantly higher occipital FDG avidity than MCI/Normal subjects, an effect preserved in the left occipital lobe with cerebellar normalization, which may represent a possible future biomarker of PPA which will be explored in future prospective studies.

*Second Prize - Dr. Hussein M. Abdel-Dayem Award

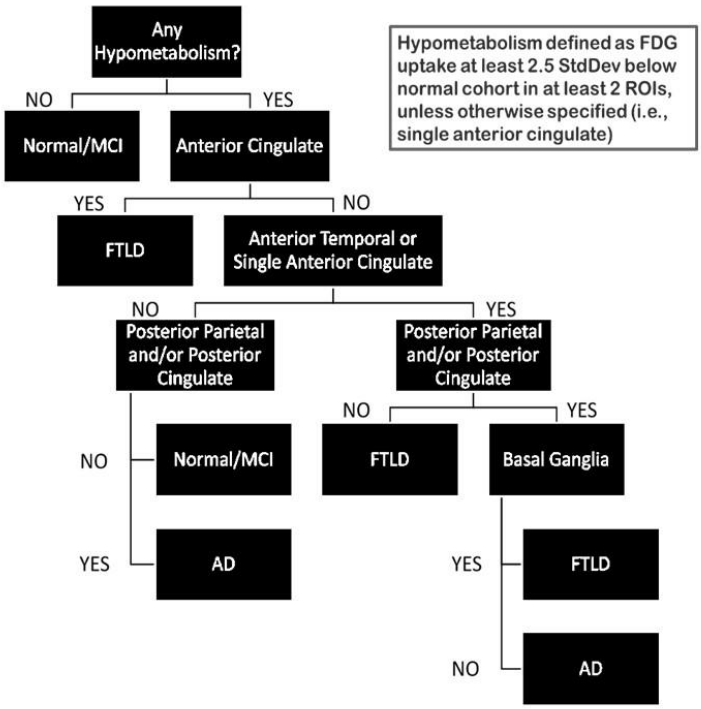
Any Hypometabolism?
NO
YES
Normal/MCI
Anterior Cingulate
Hypometabolism defined as FDG uptake at least 2.5 StdDev below normal cohort in at least 2 ROIs, unless otherwise specified (i.e., single anterior cingulate)
YES
NO
FTLD
Anterior Temporal or Single Anterior Cingulate
NO
YES
Posterior Parietal and/or Posterior Cingulate
Posterior Parietal and/or Posterior Cingulate
NO
YES
NO
Normal/MCI
FTLD
Basal Ganglia
YES
AD
YES
FTLD
NO
AD

Initial experience with ^{18}F- Fluoroglutamine PET/CT imaging for assessment of brain tumor pseudoprogression*

Reema Goel[1], Kwaku Domfe[2], Alexandra Miller[3], Elena Pentsova[3], Viviane Tabar [3], Ingo Mellinghoff [3], Christian Grommes [3], Lisa DeAngelis[3], Maya Graham [3], Robert Young[1], Mark Dunphy[1]
[1]Department of Radiology, Memorial Sloan Kettering Cancer Center, New York, NY; [2]College of Medicine, SUNY Upstate Medical University, Syracuse, NY; [3]Department of Neurology, Memorial Sloan Kettering Cancer Center, New York, NY

Background: Reliable assessment of therapeutic response and progression in brain malignancy is challenging for neurooncologists, as current standard neuroradiologic tumor biomarkers, including conventional MRI, FDG PET and FLT PET, have suboptimal diagnostic specificity. Pseudoprogression, an apparent increase in contrast-enhancing tumor volume on post-treatment MRI, is seen in a significant number of glioblastoma patients receiving chemoradiotherapy. This study highlights our initial experience evaluating the efficacy of ^{18}F- Flouroglutamine PET for distinguishing brain tumor pseudoprogression in human subjects.

Methods: 24 patients (Non gliomas: 3 brain metastases from lung cancer, 1 brain metastases from breast cancer; Gliomas: 2 low grade and 7 high grade astrocytomas, 1 anaplastic oligodendroglioma, 1 anaplastic ependymoma and 9 glioblastoma multiforme) with suspected recurrence or equivocal findings on MRI underwent ^{18}F- Fluoroglutamine PET/CT imaging before the start of new treatment in gliomas (7), within 12 weeks after completion of radiochemotherapy in gliomas (10) and after 12 weeks post completion of radiation therapy/chemoradiation including metastases (7). 13 patients also underwent ^{18}F- FDG PET/CT. Qualitative and quantitative evaluation (maximum and mean tumour-to-brain ratios (TBRmax, TBRmean) was performed. Reference standard was based on the clinical course, follow-up MR imaging and/or histopathological findings.

Results: In the glioma subgroup, ^{18}F- Fluoroglutamine PET showed sensitivity of 94% and specificity of 67% in differentiating tumor progression /presence of high grade glioma (TP=16; FP=1;TN=2;FN=1).Of 10 patients classified as having early true progression, 8 were positive on Fluoroglutamine and of 2 patients classified as true late progression both were positive on Fluoroglutamine. In non glioma subgroup, of 3 patients classified as having early/late true progression/metastases, all 3 were positive on Fluoroglutamine and 1 patient classified as negative for metastases was also negative on Fluoroglutamine

Conclusions: ^{18}F-Fluoroglutamine PET appears sensitive for diagnosis of early/late progression of brain tumor progression post-treatment.

*Third Prize - Dr. Hussein M. Abdel-Dayem Award

Analysis of different infusion techniques for Lu-177 DOTATATE for peptide receptor radionuclide therapy

Forbes S, Yahya T, Parkar F, Baghdadi Y, Paul P, Abraham T & Love C.
Division of Nuclear Medicine, Montefiore Medical Center, Bronx, NY

Background: We have used two methods of infusion of Lu-177 DOTATATE (Lu-177) for peptide receptor radionuclide therapy (PRRT) in patients with progressive neuroendocrine tumors (NET) while on conventional therapy: gravity and electric pump methods. Each has its own advantages and disadvantages. Pump method required aspiration of the radiopharmaceutical from the vial into a syringe which is then connected to the patient's intravenous (IV) access using a connector line. The dose is infused using an electronic pump programmed to infuse over 30 minutes. This process required exposure of the hands when aspirating. After infusion, the agent left within the connector is difficult to access. For the gravity method, the vial remained within the shield container and required an IV bag in addition to the connector. Activity left in the connector can be easily flushed into the patient.

Methods: Under IRB approval, 31 patients were scheduled to undergo PRRT for 4 doses every 8 weeks, 12 patients completed the therapy. There was a total of 80 infusions in this investigation. To determine the net dose administered, we measured the pre and post infusion radioactivity in the vial and connector line. The amount of net dose and residual radioactivity in the vial and connector are presented for each method.

Results: The highest pretherapy dose measured at 217 mCi while the lowest measured at 190 mCi (mean 209.7 mCi). For the pump method, residual amount in the vial ranged from 2 to 4.5 mCi. Approximately 12 mCi remained in the connector. For gravity method, the residual vial activity ranged from 0.2 to 1.8 mCi. About 0.1 mCi stayed in the connector. Monthly radiation exposure data showed no significant increase in radiation dose to the physicians administering the agent with either method.

Conclusions: PRRT of NET is safe. Despite its more tedious process of preparation, gravity method allowed higher administered dose to the patients for PRRT and for this reason, it is preferred to the pump method.

Early SPECT/CT in Gastrointestinal Bleed Scintigraphy: A Case Report Illustrating Precise Bleed Localization

Shahar Glomski, MD[1,2], Rachel Powsner, MD MPH[1,3,4]

[1]Joint Program of Nuclear Medicine, Harvard Medical School; [2]Brigham & Women's Hospital Department of Radiology; [3]VA Boston Healthcare System; [4]Boston University School of Medicine Department of Radiology

Background: Gastrointestinal (GI) bleeding has a mortality rate of 10-30% in the United States. Tagged red blood cell (RBC) scintigraphy can be used to determine whether a patient is actively bleeding, to help localize the site of bleeding, and to allow for treatment planning and risk stratification. Localization of the site of bleeding on planar images alone can be limited by absence of anatomic landmarks and overlap with activity in vessels. SPECT/CT has been shown to increase positional accuracy of GI bleed over planar imaging alone. SPECT/CT can also help distinguish between GI bleed and false positive findings, such as physiologic activity in the kidney or bladder, splenosis, non-enteric bleeding, vascular collaterals, and postoperative hyperemia.

Case Report: In this case report we illustrate the utility of early, rapid SPECT/CT acquisition performed as soon as the site of bleed is identified. The acquisition required only 10 minutes with no significant interruption in dynamic imaging, and allowed for precise identification of the bleeding site.

Discussion: Published studies and reports on SPECT/CT used in gastrointestinal bleeding studies demonstrate variable times of acquisition of the SPECT/CT study, from within 30 minutes after injection of radiolabeled tracer up to several hours after injection. Delayed acquisition can complicate the interpretation as it may be difficult to distinguish the initial site of bleed from any antegrade or retrograde movement of a collection of labeled cells.

Conclusions: Early, rapid acquisition of SPECT/CT images in a gastrointestinal bleeding study provided precise localization of the site of bleeding without significant interruption in the planar dynamic acquisition.

FDG PET/CT Imaging in Sellar Plasmacytoma: Clinical Characteristics and Differential Diagnostic Considerations

Joe Jose MD, Honglei Zhan, MD, Yuliya S Jhanwar MD, Jana Ivanidze MD PhD.
Weill Cornell Medicine - New York Presbyterian Hospital, New York, NY.

Background: Sellar plasmacytoma represents a rare entity that can mimic pituitary macroadenoma both in clinical and radiographic presentation, resulting in a high rate of misdiagnosis. Typically, sellar plasmacytomas present with neurological deficits, and less frequently, anterior pituitary hypofunction is encountered. Clinical management differs greatly between the two entities. Radiation therapy is the preferred treatment for solitary plasmacytoma, with systemic chemotherapy being the preferred approach in the setting of multiple myeloma, while surgery remains the mainstay of treatment in pituitary macroadenoma. Given these significant differences, early differential diagnosis is critical to optimize patient outcomes.

Methods: Two cases of sellar plasmacytoma in patients with known systemic multiple myeloma were presented to illustrate differential diagnostic considerations. Key FDG-PET and MRI characteristics are discussed.

Results: Case 1: A 59 year old female with known multiple myeloma presented to the emergency department with right-sided vision loss and clinical findings of right cranial nerve VI involvement. Multiple myeloma was diagnosed 6 years ago. Biopsy demonstrated 80% lambda and 5% kappa light chains consistent with osseous plasmacytoma. Whole-body FDG-PET/CT showed extensive lytic osseous lesions throughout the axial and appendicular skeleton, and an FDG-avid expansile soft tissue mass centered in the sella. Brain MRI confirmed an enhancing soft tissue mass centered in the sella, with osseous destruction of the clivus and extension into the right cavernous sinus.
Case 2: A 60 year old female with no significant prior medical history presented to the emergency department with chest pain and was found to have pancytopenia. CT revealed innumerable lytic osseous lesions with associated osseous destruction. Bone marrow biopsy demonstrated multiple myeloma, 80 % bone marrow involvement with plasma cells. Whole body FDG PET/CT showed numerous FDG-avid lytic osseous lesions, compatible with active myeloma. An intensely FDG-avid, expansile soft tissue mass with associated expansion of the sella was also seen extending to involve the left cavernous sinus and Meckel's cave.

Conclusions: Sellar plasmacytoma is a rare but important differential diagnostic consideration in patients who present with clinical and radiographic findings of sellar mass. A subset of patients present with solitary sellar plasmacytoma and subsequently develop systemic multiple myeloma; whereas another subset of patients present with sellar plasmacytoma in the setting of systemic multiple myeloma. Pituitary macroadenoma represents the most important differential diagnostic consideration. Both entities can demonstrate FDG avidity on PET imaging and therefore, pathologic correlation is ultimately needed to confirm the diagnosis. However, FDG PET/CT can help accurately assess extent of disease and aid in surgical and radiation treatment planning.

Gallium-68-DOTATATE PET/CT in the Diagnosis and Management of Gastrointestinal Neuroendocrine Tumors: A Pictorial Review

Seyed Ali Mosallaie MD, Silvina Dutruel MD, Yuliya Jhanwar MD, Honglei Zhang MD, Jana Ivanidze MD PhD.
Weill Cornell Medicine - New York Presbyterian Hospital, New York.

Introduction: Gastrointestinal neuroendocrine tumors (GNET) are a heterogeneous entity including slow-growing as well as highly aggressive presentations. Surgery is a treatment option if the diagnosis is made early, however GNET can often be asymptomatic until late in the disease course and are frequently metastatic at presentation. Molecular imaging plays an increasingly important role in both the initial evaluation and longitudinal follow-up of patients with GNET. GNET express high levels of somatostatin receptors (SSTR), most notably SSTR2A. Scintigraphic SSTR-targeted imaging has been performed over the past 35 years with Indium-111-Octreotide, however this approach is limited given the relatively low resolution, limited specificity, cumbersome logistics with imaging over multiple days, and significant radiation dose. ^{68}Ga DOTATATE PET/CT has a favorable half-life, excellent specificity and sensitivity, improved patient convenience, and a lower effective dose compared to Indium-111-Octreotide, and has entered clinical practice in the management of GNET in recent years. Furthermore, Lutathera has recently received FDA approval for radionuclide therapy of GNET, after the prospective multi-center clinical trial, NETTER-1, demonstrated improved clinical outcomes. We present two illustrative cases where ^{68}Ga DOTATATE PET/CT was useful in the longitudinal follow-up and treatment response monitoring in patients with GNET.

Case 1: A 69 year-old male with no significant past medical history presented with severe abdominal pain, nausea and vomiting and was found to have a partial small bowel obstruction. Initial CT revealed multiple peripherally enhancing hepatic lesions suspicious for metastatic disease, and biopsy confirmed metastatic well-differentiated neuroendocrine tumor, WHO Grade 2. Subsequent ^{68}Ga DOTATATE PET/CT revealed a mass in the body of the pancreas, multiple lymph nodes above and below the diaphragm, as well as foci in the left ventricle, gastric body, liver, and subcutaneous soft tissues. Lanreotide therapy was subsequently initiated. Follow-up ^{68}Ga DOTATATE PET/CT 3 months after therapy initiation demonstrated interval decrease in avidity of the aforementioned lesions.

Case 2: An 81 year-old female presented with post-prandial right-sided abdominal pain, and initial imaging revealed a small right lower quadrant mass. The patient underwent a laparotomy, small bowel resection with primary anastomosis, resection of omental, diaphragmatic, and ovarian nodules with pathology demonstrating a well-differentiated neuroendocrine neoplasm, intermediate grade. ^{68}Ga DOTATATE PET/CT demonstrated numerous intensely DOTATATE-avid hepatic and osseous lesions, as well as a DOTATATE-avid lymph nodes above and below the diaphragm. The patient underwent therapy with Lanreotide and Denosumab. Follow up Ga-68 DOTATATE PET/CT six months after initiation of therapy demonstrated a mixed interval response, with some hepatic lesions demonstrating interval increase in DOTATATE avidity, while some lymph nodes and osseous lesions demonstrated interval decrease. A second follow-up ^{68}Ga DOTATATE PET/CT 4 months later demonstrated increased confluence of DOTATATE-avid hepatic foci, as well as new and increased DOTATATE-avid retroperitoneal lymph nodes and osseous lesions. The patient is currently undergoing therapy with Lutathera.

Conclusion: ^{68}Ga DOTATATE PET/CT plays an increasingly important role in the diagnosis and treatment response monitoring of metastatic GNET, allowing for accurate staging and optimized patient selection for therapy with Lutathera.

Ability of Renal Function Tests to Predict ^{131}I Empiric Dose

Kenneth J Nichols PhD; Maria B Tomas MD; Gene G Tronco MD; Fritzgerald C Leveque LNMT; Kuldeep K Bhargava PhD; Christopher J Palestro MD
Department of Radiology, Donald and Barbara Zucker School of Medicine at Hofstra/Northwell, New Hyde Park, NY.

Background: In order to limit radiation dose to blood < 200 cG for pts receiving ^{131}I to treat thyroid cancer, reasons to first assess ^{131}I uptake prior to therapy include abnormal renal function (AbnlRF). There are several tests available to determine whether pts have AbnlRF. Our study was conducted to determine if there is a particular test, or combination of tests, that accurately predicts which pt would receive excessive dose if administered an empiric ^{131}I activity of 200 mCi.

Methods: Data were examined retrospectively for 100 pts undergoing initial ^{131}I uptake evaluation following administration of 1-4 mCi ^{131}I. ^{131}I blood-measurement-only dosimetry of blood samples collected over 5-7 days (J Nucl Med 2017;58:1588-95) was used to compute dose to blood. Each pt had blood urea nitrogen (BUN) & creatinine (CR) laboratory results, including indications whether their results exceeded normal limits established individually by each laboratory. In addition, estimated glomerular filtration rate (eGFR) adjusted for age & gender was computed as eGFR = $\exp(1.911+5.249/CR - 2.114/CR^2 - (0.00686 \times age) - r)$, where r = 0.0 for males & 0.205 for females (if CR < 0.8 mg/dL, 0.8 mg/dL was used), for which the lower limit of normal is 63 mL/min/1.73 m^2 (Ann Intern Med 2004;141:929–37).

Results: Agreement among the 3 tests as to whether or not a pt had AbnlRF ranged from "good" to "excellent" between BUN & eGFR ($\kappa = 0.69$), BUN & CR ($\kappa = 0.77$), & CR & eGRF ($\kappa = 0.92$). 26 pts had AbnlRF by BUN, 27 by CR, & 26 by eGFR. Identifying pts for whom dose would be excessive was predicted with similar accuracy (75%, 72% & 70%), sensitivity (62%, 59% & 55%), & specificity (89%, 86% & 86%) by BUN, CR & eGFR, respectively. In the 20 pts for whom all 3 blood tests indicated AbnlRF, 70% would have had excessive radiation dose if administered 200 mCi ^{131}I; 40% would have had excessive dose if administered 150 mCi ^{131}I. Predicted dose did correlate significantly ($p < 0.007$) with BUN, CR & eGFR ($r = 0.48, -0.48$ & 0.27), but differences were substantial between dose predicted from renal function versus as measured from multiple blood samples (18%, 37% & 18%, respectively).

Conclusions: Even when all blood tests indicate AbnlRF, not all pts would receive an excessive radiation dose to blood if administered an empirical activity of 150-200 mCi ^{131}I. Therefore, it is important to perform ^{131}I dosimetry measurements on all pts with AbnlRF before beginning ^{131}I radiation therapy for thyroid cancer.

Thyroidectomy and I-131 Radioiodine Therapy in a Case of Persistent Disseminated Benign Struma Ovarii

Laura Ortiz-Teran MD PhD[1,2], Najmosama Nikrui MD[3,4], Rachel Powsner MD MPH[1,3,5]
[1]Joint Program of Nuclear Medicine, Harvard Medical School; [2]Brigham & Women's Hospital Department of Radiology; [3]Boston VA Healthcare System; [4]Gynecology and Reproductive Biology, Harvard Medical School, Massachusetts General Hospital; [5]Boston University School of Medicine Department of Radiology

Background: Teratomas are germ cell tumors that can contain several different types of tissue such as bone, hair, and muscle. Mature teratomas (those in which the component cells are more identifiable as a specific type of tissue) contain some thyroid tissue in 5-20% of cases. Struma ovarii is defined as a mature ovarian teratoma containing at least 50% normal thyroid tissue or containing any quantity of malignant thyroid tissue (most commonly papillary thyroid cancer). Struma ovarii is relatively rare, accounting for approximately 1% of all ovarian teratomas. The effective treatment of benign teratoma is unilateral salpingo-oophorectomy or ovarian cystectomy. Malignant transformation of the thyroid tissue in struma ovarii occurs in 5-15% of the cases and treatment of these cases include hysterectomy and bilateral salpingo-oophorectomy. Adjuvant therapy with thyroidectomy and follow-up I-131 radioiodine therapy is reported in cases with malignancy and in a few cases of recurrent benign disease.

Case Report: We present a case of benign struma ovarii in a middle-aged women with intermittent recurrent episodes of abdominal pain over 20 years requiring multiple surgeries to remove intraperitoneal tumor implants even after completion of bilateral salpingo-oophorectomy and hysterectomy. She had effective resolution of her symptoms following each procedure. I-123 whole body imaging and an intraoperative probe were used in several of the more recent surgeries to locate and remove stromal implants. After the most recent surgery the patient was willing to have thyroidectomy and I-131 radioiodine therapy. The patient was then treated with I-131 radioiodine.

Discussion: I-123 imaging performed immediately prior to I-131 radioiodine therapy as well as I-131 imaging one week following treatment demonstrated many more thyroid tissue deposits post thyroidectomy compared to the pre-thyroidectomy I-123 scans. This could mean that there were new lesions or persistent small lesions that could not be adequately visualized or removed due to their relatively low iodine uptake in the presence of an intact thyroid gland. It has been hypothesized that some pathologically benign struma ovarii may demonstrate potentially malignant characteristics; in one of the previously reported cases of benign struma ovarii aggressive biologic behavior of the tissue was hypothesized to be due in part to the presence of increased expression of vascular endothelial growth factor (VEGF) and p53 protein.

Conclusions: This case demonstrates the rarely reported role of thyroidectomy and I-131 therapy in the treatment of recurrent and/or persistent disseminated benign struma ovarii. Many pre-existing or recurrent lesions become apparent on I-123 imaging and amenable to I-131 therapy following thyroidectomy.

Utility of Gallium-67 Citrate SPECT-CT in the Evaluation of Infection of Left Ventricular Assist Devices

Fauziya Parkar MD[1], Aileen Tlamsa MD[2], Justin Nistico MD[2], Victoria A Muggia MD[2], Grace Y Minamoto MD[2], Renee M Moadel MD[1], Yoram A Puius MD PhD[2]
[1]*Division of Nuclear Medicine; Montefiore Medical Center, Bronx, NY.*
[2]*Department of Infectious Disease, Montefiore Medical Center, Bronx, NY.*

Introduction: Left ventricular assist device (LVAD) can be used as bridge to cardiac transplant or as long-term destination therapy for patients with end-stage heart failure. However, device related infection (DRI) is common complication, and nuclear medicine studies are useful for localizing and determining the extent of DRIs. Different parts of the device can become infected, and each is associated with different clinical and surgical management. Gallium-67 citrate SPECT-CT (Ga67) is one of the modalities utilized to detect LVAD DRI, and is more available and of lower cost than labeled WBCs and FDG-PET at our institution. As a consequence, Ga67has become the de facto standard modality in determining the presence and anatomical extent of LVAD DRI at Montefiore, and we report our experience.

Objective: To evaluate the utility and clinical consequence of Ga67 in patients with suspected LVAD DRI.

Methods: A retrospective analysis was performed from Jan2011 to June 2018 of all patients with LVAD who underwent Ga67. Clinical and laboratory data were collected for each patient: age, sex, outcome: continued antibiotics, surgical management, LVAD explant, heart transplant, death.

Results: 40 patients with LVADwere identified (11 patients had repeat Ga67 scans), age range of 23 to 76 years, 32 males and 8 females.19 patients had no evident of infection on Ga67 and were treated medically by surface drainage and with shorter course of oral antibiotics.21 patients had LVAD DRI detected on Ga67: 17 driveline, 2 device infections, 2 inflow/outflow conduit. Patients with infected drivelines underwent surgical washout or repositioning and IV antibiotics. Patients with inflow/outflow conduit infections were treated with IV antibiotics andsurgical washout.Patients with device infections were treated with IV antibiotics, surgical washout and/or surgical device exchange. 16 patients eventually underwent cardiac transplantation.

Discussion: This is the largest series of Ga67 scans for evaluation of infection in patients with LVAD. Ga67 detected the presence and extent of infection, and aided in medical and surgical therapeutic management.

Role of Bone Scan in the Era of PET/CT Patients with Sarcoma

F Parkar, T Abraham, R Moadel, C Love.
Division of Nuclear Medicine, Department of Radiology, Montefiore Medical Center, Bronx, NY

Objective: For imaging of patients with sarcoma, MRI or contrast enhanced CT are preferred. Due to its exquisite sensitivity, FDG PET/CT (FDG) is commonly employed for initial and subsequent treatment strategy. However, conventional MDP bone scan (BS) is still used in this patient population. This study was undertaken to re-evaluate the role of BS in the era of PET/CT.

Methods: Following local IRB approval, images of 19 anonymized patients who underwent BS at diagnosis of sarcoma were reviewed by 2 nuclear medicine physicians who did not have any knowledge of final staging or results of other imaging. There were 9 cases of Ewing's and 10 cases of osteosarcoma in 6 females and 13 males, aged 7 to 54 years. Nine of the 19 patients also underwent FDG. Focal abnormal activity at the sight of known malignancy and in other osseous structures was considered (+) for malignant lesion. Imaging results were compared with final diagnoses based on histopathologic examinations, other collaborating morphologic imaging and institutional final impression.

Results: Primary lesion in 18/19 patiens were true positive (TP) on BS with sensitivity of 95%. The false negative (FN) result on BS was also FN on FDG; histopathologic examination in this case showed round blue cell neoplasm with extensive necrosis including in the bone. The rest of the 8 cases imaged with FDG were TP.
For detection of distant metastases, BS was TP (n=9); true negative (TN) (n=10). FDG was TP (n=2); TN (n=6) and FN (n=1). FN was seen in a patient with lesions in bones of a knee joint which was interpreted as one lesion. FDG, as expected, was able to detect lung and nodal metastases.

Conclusions: Detection of osseous metastasis is important for treatment planning in patients with sarcoma. In this patient population, BS was able to detect distant metastasis with high degree of accuracy allowing planned treatment to proceed.

Comparison of SPECT-CT Pre-Treatment ^{99m}Tc-MAA and Post-Treatment ^{90}Y Glass Microspheres Dosimetry Estimates and Hepatocellular Carcinoma Tumor Response

Rachel Powsner MD[1,2], Joseph Darman CHP[1], Ducksoo Kim MD[1,2], Anupma Jati MD[1,2]
[1]Boston VA Healthcare System, [2]Boston University School of Medicine

Introduction: Accurate estimation of dosimetry for ^{90}Y microsphere treatment of hepatic malignancies is limited by physical and imaging characteristics of ^{99m}Tc-MAA and ^{90}Y microspheres. The 140keV photons from ^{99m}Tc-MAA permit better lesion edge detection than the broad spectrum ^{90}Y bremsstrahlung radiation. The pattern of distribution of the ^{99m}Tc-MAA in the liver is often different than that of the ^{90}Y microspheres. Particle size and morphology differences may in part explain this difference, PET-CT imaging of the small yield of positron emissions in the decay scheme of ^{90}Y allows much better image quality. However, this modality is not as available as SPECT-CT.
In this study the estimated tumor dosimetry from pre-treatment ^{99m}Tc-MAA imaging was compared with estimates from post treatment ^{90}Y bremsstrahlung imaging. Tumor response based on follow up imaging was compared to dosimetry estimates for both types of imaging.

Methods: All patients were enrolled in the ^{90}Y glass microsphere treatment IRB protocol. Imaging and data from all patients receiving treatment for hepatocellular cancer from the period of 8/2/16 to 6/28/17 were included. Using visual comparison of pre-treatment contrast enhanced CT or MRI imaging with ^{90}Y ^{99m}Tc-MAA and post-treatment ^{90}Y bremsstrahlung imaging regions of interest were drawn around areas of hyperemia corresponding to tumors. Counts and volumes calculated from the regions were used to estimate dosimetry based on standard formulas. Follow-up CT or MRI images were reviewed for any evidence of tumor response.

Results: 19 distinct hyperemic lesions in 12 patients were identified. 10 of these lesions could also be identified on MAA imaging. Calculated tumor doses on ^{90}Y bremsstrahlung imaging ranged from 112-605 Gy (319 ± -159 Gy). Calculated pre-treatment tumor doses from ^{99m}Tc MAA imaging ranged from 100 to 874 Gy (474 ± 239 Gy). There was no significant correlation between the ^{90}Y bremsstrahlung and ^{99m}Tc MAA tumor doses (correlation coefficient of 0.2). Of the 19 lesions 12 had at least one follow-up CT or MRI image; all tumors demonstrated partial or complete response. There was no significant correlation between degree of response and dosimetry for either ^{90}Y bremsstrahlung or ^{99m}Tc-MAA imaging (correlation coefficients of 0.22 and 0.37).

Discussion: Although there was no significant correlation between calculated dosimetry of ^{99m}Tc-MAA pre-treatment and ^{90}Y bremsstrahlung post treatment imaging there were inherent limitations in the study including small sample size and qualitative determination of tumor boundaries based on local hyperemia and visual inspection of contrast enhanced anatomical imaging. In concurrence with pre-existing literature, the cases in this study frequently demonstrated a discrepancy of distribution of the MAA and microspheres in the tumors (and the lungs). Tumor response, either partial or complete, was noted in all cases regardless of administered dose or calculated dosimetry.

Conclusions: There was no evidence of correlation between dosimetry estimates derived from SPECT-CT pre-treatment ^{99m}Tc-MAA and post-^{90}Y glass microsphere treatment bremsstrahlung imaging. Tumor response, either partial or complete, was noted regardless of administered dose or calculated dosimetry.

Benefits of Interpreting PET/CT in a Multidisciplinary Environment

JN Rini, GG Grimaldi, N Rahmani, E Ben-Levi
Department of Radiology, Donald & Barbara Zucker School of Medicine at Hofstra/Northwell, Hempstead, New York

Objective: To illustrate the benefits of interpreting PET/CT in a multidisciplinary reading room where there is a culture of cooperation and collaboration.

Background: PET/CT is a powerful diagnostic imaging technique that plays a vital role in the evaluation and management of certain malignancies. It may detect metastatic disease that is not detectable or overlooked on conventional imaging studies, and it may expedite the diagnosis and staging of disease by delineating a lesion that is accessible to image-guided biopsy, thus obviating the need for an invasive, more costly procedure. Rendering a useful, clinically relevant PET/CT report requires knowledge of patient history, the clinical question being asked, and an understanding of how the scan results will impact patient management. Correlation with prior PET/CT scans and diagnostic CT, MRI and ultrasound examinations is essential. Consultation with subspecialty trained radiologists may provide invaluable assistance in clarifying abnormalities seen on correlative imaging studies, as well as aid in the diagnosis of abnormalities which may be retrospectively identified utilizing PET/CT. It also aids in the identification of the most appropriate lesion to biopsy and the most suitable image-guided approach. Collaboration also may facilitate the identification of infectious and inflammatory conditions that can mimic malignancy. In this era of increasing workloads and emphasis on productivity, consultation with colleagues, while professionally rewarding, can be challenging due to time and geographic constraints.

Methods: At our center PET/CT scans are read by a nuclear medicine physician in a multidisciplinary reading room that includes subspecialty trained chest and body radiologists with combined expertise in reading diagnostic CT, MRI and ultrasound studies and performing CT and ultrasound-guided biopsies, thoracentesis and paracentesis. Neuro, musculoskeletal and pediatric radiologists are available for remote consultation. Physicians consult with each other as needed when studies are read and when procedures are performed. Biopsy results are discussed and images are re-reviewed to verify concordance.

Results: The benefits of the multidisciplinary reading room are illustrated in our series of cases which show (1) how lesions identified for ultrasound-guided biopsy on FDG-PET/CT led to the diagnosis of newly diagnosed metastatic lung adenocarcinoma, recurrent ovarian carcinoma, recurrent metastatic esophageal cancer, and sarcoidosis; (2) an Axumin-avid lytic metastasis retrospectively seen on diagnostic CT; (3) a DOTATATE-avid neuroendocrine tumor of terminal ileum with unsuspected lymph node and liver metastasis; (4) malignancy mimics including FDG-avid umbilical and inguinal hernia plugs and infected dropped gallstones/ventral hernia mesh.

Conclusions: The multidisciplinary, collaborative reading room is a professionally rewarding environment which fosters continued education amongst peers and imparts more meaning to the diagnostic process. This setting potentially leads to more accurate PET/CT reports and expedited, more cost-effective patient care. Our experience highlights the benefits and value added by this environment.

Gallium-68-DOTATATE PET/MRI in the Diagnosis and Management of Meningiomas: A Case Series

M Roytman[1], RS Magge[2], DJ Pisapia[3], PE Stieg[4], TH Schwartz[4], A Gupta[1], SP Dutruel[1], NA Karakatsanis[1], SA Nehmeh[1], JR Osborne[1], SC Pannullo[4], J Ivanidze[1]
[1]Department of Radiology, Weill Cornell Medical College, New York-Presbyterian Hospital, NY, NY, USA; [2]Department of Neurology, Weill Cornell Medical College, New York Presbyterian Hospital, NY, NY, USA; [3]Department of Pathology, Weill Cornell Medical College, New York Presbyterian Hospital, NY, NY, USA; [4]Department of Neurological Surgery, Weill Cornell Medical College, New York Presbyterian Hospital, NY, NY, USA

Background: Meningiomas are the most common primary intracranial tumors, typically treated with surgery and adjuvant radiation in cases of subtotal resection and/or higher histopathologic grade. Contrast-enhanced MRI is the gold standard for postoperative assessment and adjuvant treatment planning. However, MRI can have limited sensitivity and specificity in cases of infiltrative lesions, osseous or parenchymal invasion, and postsurgical or postradiation change. Ga-68-DOTATATE is a PET radiotracer targeting somatostatin receptor 2 (SSTR2) and has recently entered clinical practice for the diagnosis and treatment response assessment of gastrointestinal neuroendocrine tumors. Meningiomas express high levels of SSTR2, thus SSTR-targeted PET/CT can be utilized in the detection, target volume definition, and assessment of osseous invasion in meningiomas. To date, the role of Ga-68-DOTATATE PET/MRI in meningioma has not been explored.

Methods: IRB approval with waived consent was obtained for this retrospective, HIPAA compliant case series of 8 consecutive patients with a history of meningioma in whom Ga-68-DOTATATE PET/MRI was obtained for the clinical purposes of differentiating recurrent meningioma from posttreatment change. PET/MRI was performed on the Biograph mMRTM scanner (Siemens Healthineers, Erlangen, Germany) or the GE SIGNATM PET/MR scanner (GE Healthcare, Milwaukee, WI). PET imaging started at 15 min post-injection of approximately 5 millicuries of Ga-68- DOTATATE. PET data were acquired in 3D List Mode for a total of 40 minutes, to allow for both static and dynamic PET data analysis. The list mode PET data was replayed retrospectively to reconstruct the last 10 min data set (i.e. at a single static frame 45 to 55 min post-injection). MR imaging was performed according to institutional protocol and MR based attenuation correction was obtained according to manufacturer's standard-of-care specifications. Two patients, who were ineligible for PET/MRI, underwent PET/CT and MRI separately.

Results: We present a series of 8 cases demonstrating the utility of Ga-68-DOTATATE PET/MRI in assessing the extent of disease in patients with pathology proven or presumed meningioma. Specifically, Ga-68-DOTATATE PET/MRI distinguished recurrent meningioma from adjacent posttreatment/postradiation change, confirmed osseous invasion, identified additional meningiomas not previously identified on contrast-enhanced MRI and confirmed the presence of a meningioma in a case in which hemangiopericytoma had been in question.

Conclusions: Ga-68-DOTATATE PET/MRI demonstrates utility in the diagnosis and management of meningiomas, ultimately aiding in targeted short interval follow-up and treatment planning.

Nuclear Medicine Report Addenda: A Quality Improvement Project of 18,343 Nuclear Medicine Studies Over 5 Years

Jay Sangani MD, Sara Venezia DO, Humza Haque, Jeffrey S Kempf MD FACR
Rutgers-Robert Wood Johnson Medical School

Introduction: This quality improvement study aims to identify the etiology of all nuclear medicine addenda over a five year period to aid in our report communication with referring physicians. We categorized etiologies for addenda creation and evaluated methods to decrease future NM report addenda creation with purpose to improve future patient outcomes if found to be adversely affected.

Methods: Our retrospective review was performed utilizing a data mining software, Montage, searching for "addendum" in the Nuclear Medicine (NM) category over a 5 year period from January 1, 2013 through January 31, 2018 of 18,343 NM studies performed at a single tertiary care referral hospital. This study was IRB exempt. We evaluated and categorized the etiology of NM addenda, time to addenda creation, as well as potential minor versus major clinical impact of NM addendums.

Results: Of the 18,343 nuclear medicine studies reported, 346 reports contained the keyword "addendum" with an overall frequency of 1.9%. Of these 346 addenda, 68 reports did not meet inclusion criteria for the study: reports contained the word "addendum" but were not addended, contained an addendum issued at the time of the original report, or they were addended for quality assurance and billing purposes. Of the remaining 278 reports containing "addendum": 13 etiology categories were created; an addendum could be multifactorial and Boolean flag set each qualifying category resulting in 345 selected factors in 278 addenda (1.24:1). The 5 most common etiologies for nuclear medicine addenda were for typographical errors (28.4%), clarification of previously described finding (20.1%), communication with referring clinician (19.4%), additional or delayed imaging performed (14.4%), and structured reporting error (14.0%). Of the 278 addenda, 8.6% were deemed to have potential for major/significant impact on patient care. Subsequent chart review revealed no significant adverse patient outcomes. The temporal relationship between completion of the original report and subsequent addendum creation as follows: 16.5% within 10 minutes; 41.0% within 1 hour, 79.1% within 24 hours, 94.2% within 7 days.

Conclusions: Overall, there was a low frequency of 1.9% of nuclear medicine addenda in this study. Common categories for addenda creation including typographical errors (28.4%) and correction of structured reporting errors (14%), which could potentially be avoided with use of a revisionist. 16.5% of addenda could be avoided by elongating time to finalization of report completion to ten minutes. 91.4% of addenda had potential minor or no clinical impact in this study and no significant adverse patient outcomes found on chart review.

^{18}F-FDG Uptake in Uninfected Aorto/iliac Endovascular Grafts

Maria-Bernadette S Tomas MD; Meera Raghavan MD; Kenneth J Nichols PhD; Christopher J Palestro MD.
Donald and Barbara Zucker School of Medicine at Hofstra/Northwell, New Hyde Park, NY.

Objectives: Although 18F-FDG has been used to diagnose infected prosthetic vascular grafts, uptake of this radiopharmaceutical in uninfected grafts can potentially confound study interpretation. Our investigation was undertaken to analyze uptake of 18F-FDG in uninfected aorto/iliac endovascular grafts and determine whether this uptake changes over time.

Methods: Pts with aortic endovascular grafts who underwent serial ^{18}F-FDG PET/CT imaging for oncologic indications were identified from the departmental database. A single nuclear physician scored impression of graft visibility on a 4-level scale (0 = no; 1 = diffuse homogenous without focal uptake; 2 = diffuse homogenous with focal uptake; 3 = diffuse heterogenous without focal uptake). The same physician measured maximum & mean SUV values at 3 locations along the graft & in a background region of the ascending thoracic aorta. Ratios of maximum graft to maximum background & of mean graft to mean background SUV were computed. Differences between graft & background values compared to initial values were assessed for each pt by the unpaired t-test. Linear regression tested whether there were any pts for whom graft-to-background ratios changed over time.

Results: 88 ^{18}F-FDG PET/CT scans performed on 24 pts (6 female; 18 male; age: 74±10 yrs; range: 63 - 90 yrs) were included in this retrospective investigation. The graft extended into the right iliac artery in 23 pts and into the left iliac artery in 22 pts. Eight pts had 2 scans, 8 pts had 3, 1 pt had 4, 2 pts had 5, 3 pts had 6, 1 pt had 7 & 1 pt had 8 scans. Age of grafts was 55±37 months (range: 2 – 163 months). 204 aortic grafts & 305 iliac grafts were scored "0," 51 & 168 were scored "1," while 9 & 12 were scored "3." Graft SUV's were higher for those scored "3" compared to those scored "0" or "1" (2.74±0.39 versus 1.80±0.38, $p < 0.0001$), as were background SUV's (2.50±0.23 versus 1.84±0.32, $p < 0.0001$), so that graft-to-background SUV ratios were similar (1.11±0.20 versus 0.99±0.20, $p = 0.08$). 15 graft SUV values were significantly higher & 23 were lower than 420 background SUVs, consistent with 95% of graft SUV values falling within 2 standard deviations of mean background SUV values, as expected for normally distributed graft & background SUV values. All aortic & iliac graft-to-background SUV ratios were normally distributed (Kolmogorov-Smirnov $p > 0.10$) and were consistent with a mean value of 1.0 for ratios of maximum values (1.16±0.25) and for ratios of mean values (0.99±0.20). Maximum graft SUV was significantly correlated with maximum background SUV for aortic grafts ($r = 0.57$, $p < 0.0001$) & for iliac grafts ($r = 0.37$, $p < 0.0001$), & mean graft SUV was significantly correlated with mean background SUV for aortic grafts ($r = 0.51$, $p < 0.0001$) & for iliac grafts ($r = 0.29$, $p < 0.0001$). Linear regression indicated that there were no cases of significant changes over time for maximum graft-to-maximum background SUV ratios for any of the grafts $p > 0.05$), nor for mean graft-to-mean background SUV ratios for aortic grafts or iliac grafts ($p > 0.05$).

Conclusions: ^{18}F-FDG in uninfected aorto/iliac endovascular grafts is indistinguishable from ^{18}F-FDG uptake in background tissue, and neither increases nor decreases significantly over time.

SPECT Myocardial Perfusion Imaging, a Comprehensive Educational Case-Based Review

Louis P Zingas[1], Nathaniel T Yohannes, [2], Nicholas P Zingas[2], Marques L Bradshaw MD[3,4], Chirayu Shah MD[3,4]
[1]Boston University School of Medicine;[2] Vanderbilt University School of Medicine; [3] Department of Medical Imaging, Tennessee Valley Healthcare, Nashville, TN, USA; [4] Department of Radiology, Vanderbilt University Medical Center, Nashville, TN, USA

Introduction: Myocardial perfusion imaging (MPI) is a powerful imaging modality used to evaluate, diagnose, and triage various cardiovascular disease processes. We present a comprehensive educational case-based exhibit showcasing a variety of coronary pathologies, commonly seen artifacts, and rare disease processes seen on MPI.

Case Descriptions: Nine cases are presented, each demonstrating a classic pathology, artifact or disease process. Each case includes images and pertinent history from patients who underwent single-photon emission computed tomography (SPECT) myocardial perfusion imaging at both Vanderbilt University Medical Center and the Nashville Veteran's Affairs Hospital.
The first case is that of a typical myocardial perfusion imaging study featuring LAD ischemia. The patient's follow up MPI study, post-PCI, highlights key areas of revascularization.
The second case demonstrates characteristic myocardial perfusion images of triple vessel disease and highlights key features of vessel collateralization and relative blood flow commonly seen in these patients.
The third case highlights transient ischemic dilation (TID) as seen on MPI. We discuss how sub-endocardial ischemia can cause the relative appearance of dilation when utilizing this specific imaging modality.
The fourth case demonstrates what appears to be left ventricular free wall ischemia in the setting of chest pain, but is in fact dextrocardia. This case also aids the learner in identifying characteristics of situs inversus on MPI.
The fifth case showcases the effects of misregistration on myocardial perfusion imaging and how improper alignment can be misinterpreted as decreased perfusion.
The next few cases demonstrate common gastrointestinal abnormalities that can distort myocardial perfusion imaging such as ascites, hemidiaphragmatic elevation, and a gastric pull-through operation.
The final case highlights a patient who presented with chest tightness and ECG changes. Subsequent SPECT MPI demonstrated diffuse hypointensity throughout the myocardium. Follow-up CT imaging revealed a pericardial effusion.

Conclusions: Our presentation seeks to serve as an educational resource for training medical students, nuclear medicine technologist students, residents and nuclear medicine technologists with regards to myocardial perfusion imaging.

Targeted Clinical Study with 188 Re P2045 in lung cancer expressing SSTR and well differentiated Neuroendocrine tumors

Christopher P Adams[1], Ajit Shinto[2], Muhammad Wasif Saif[3]
[1]Andarix Pharmaceuticals, USA; [2]Dept. Nuclear Medicine, Kovai Medical Center, India; [3]Dept. Oncology, Tufts Medical School, USA

Background: Despite recent advances in cancer therapy, there continues to be significant medical need for molecular level targeted cancer treatments. Peptide receptor targeted radiotherapy is a selective therapeutic approach demonstrated to be effective in the treatment of certain solid tumors. Labeling targeting peptides with radionuclides can achieve both noninvasive diagnosis and targeted radiotherapy, which is the essence of theranosis. Somatostatin receptor subtype 2 (SSTR2) is widely up-regulated in many lung cancers, well differentiated neuroendocrine tumors (NETs) as well as in tumoral (but not mature) vasculature. To evaluate the biodistribution, efficacy, and safety of Rhenium 188 Re P2045, a radiolabeled somatostatin analog specific for SSTR2, to both image and treat lung cancer and neuroendocrine tumors in patients overexpressing the somatostatin receptor, a phase I trial of was performed.

Methods: In an open label, single arm study, refractory lung cancer and metastatic neuroendocrine tumor patients were first identified by image analysis. 25 Patients received an imaging dose of 7-10mCi of 188 Re and 265ng of peptide by intravenous injection. Three patients were selected, based on high SSTR expression levels, to receive a therapeutic dose of 30-50 mCi of 188 Re P2045 within 14 days after imaging. Patients were followed for 12 weeks post treatment.

Results: Imaging revealed a high density of somatostatin receptor expression in well differentiated NETs of patients. Images obtained using 188 Re P2045 demonstrated accurate detection of lung cancers with SSTR expression in a subset of patients with refractory lung cancer. The scans obtained with 188 Re P2045 were of sufficiently high quality to enable identification of receptor expression at the tumor site (Figure 1). Image-based analysis revealed that patients who received the therapeutic dose of 188 Re P2045 had a reduction in tumor mass compared to patients receiving the standard of care. No adverse events or signs of toxicity were reported by patients in either the imaging or treatment group.

Conclusions: This trial demonstrates that Rhenium 188 Re P2045 can be used safely and efficaciously to both identify and treat patients with lung cancers and neuroendocrine tumors overexpressing SSTR.

Fig 1: Comparative whole body 188 Re P2045 and 18F FDG PET CT images in 2 patients with lung cancer. The FDG PET CT images were acquired after 45-60 minutes post injection of a standard IV dose, while the 188 Re P-2045 images were acquired at two different imaging time points for dosimetric purposes. The 1st patient demonstrates very strong FDG uptake in the lung mass with hardly any SSTR expression, while the 2nd patient demonstrates strong FDG uptake as well as high grade SSTR uptake with increasing intensity over time and uptake greater than the liver by 24 hours

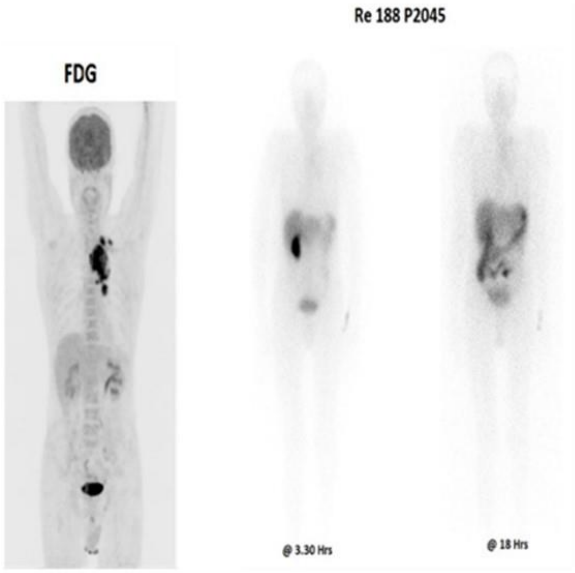

Patient 1- No SSTR expression

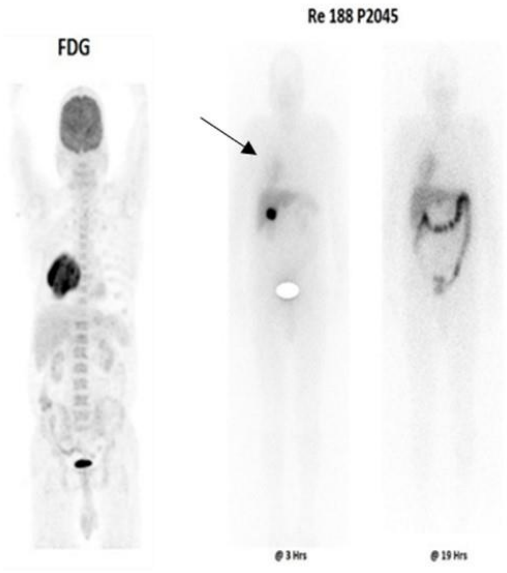

Patient 2- SSTR expression